

# Electron Microscopy to visualize T4 bacteriophage interactions with *Escherichia coli* strain DFB1655 L9, an isogenic derivative of strain MG1655 engineered to express O16 antigen

Gregory Morgan, David Lim, Paaksum Wong, Blake Tamboline

Department of Microbiology and Immunology, University of British Columbia, Vancouver, British Columbia, Canada

**SUMMARY** Research into the interaction between bacteriophage and bacteria has been a subject of interest since their discovery more than a century ago. This field has seen a resurgence in recent years because of its potential implications in the realm of medicine. Recent studies have shown that a substrain of *Escherichia coli* with O16 antigen present on their outer membrane are resistant to T4 and T7 bacteriophage-induced lysis, whereas its O16 antigen-absent counterpart is relatively more vulnerable to lysis. However, how this heightened level of resistance is achieved remains unclear. The aim of this study was to observe how the expression of O antigen affects T4 bacteriophage interactions with *E. coli* strain K-12. To do this we used wild type *E. coli* MG1655, which does not express O antigen, and isogenic strain DFB1655, into which the *wbbL* gene was introduced to restore the expression of O antigen. A control strain bearing a deletion of the outer membrane porin, OmpC, was used as a control since T4 is known to use it as a receptor. Transmission electron microscopy (TEM) was used to observe T4 bacteriophage on the surface of *E. coli*. *E. coli* substrains possessing O16 antigen had little or no adhered bacteriophage, whereas *E. coli* without O16 antigen had numerous visible bacteriophages adhered to their surface. In addition, bacterial lysis in the presence of T4 bacteriophage was monitored over time by taking optical density measurements in a lysis assay. When T4 bacteriophage was allowed to infect for an extended period of time, substrains possessing O16 antigen exhibited lower rates of lysis compared to those lacking O16 antigen. Our observations indicate that the presence of O16 antigen on the surface of *E. coli* confers protection against T4 bacteriophage-induced lysis, likely through reduced interactions with the cell surface. However, O16 antigen does not appear to provide complete immunity to phage adsorption, but rather protection that delays infection.

## INTRODUCTION

The cell envelope of gram-negative bacteria is composed of three principal layers: the outer membrane (OM), peptidoglycan cell wall, and the cytoplasmic or inner membrane (IM) (1). The outer layer of the OM is composed of lipopolysaccharide (LPS) which is the primary site of adsorption for bacteriophages (1,2). LPS attached to the surface of the OM is composed of lipid A, a polysaccharide core, and an extended polysaccharide chain called the O-antigen (1). The O antigen of *Escherichia coli* is an antigenically variable oligosaccharide polymer of repeating subunits and is present at the most external portion of the LPS molecule (3). The O antigen is one of the most variable cell constituents since the types of sugars and their respective arrangements varies greatly within strains (4). Due to its high variability, O antigen is believed to play an important role in the maintenance of bacterial diversity (4). Previous research has revealed that O antigen can serve as adsorption points for specific bacteriophages, where in other cases, the O antigen has proven to be a protective mechanism against T4 infection (5, 6)

T4 bacteriophage is one of the seven *E. coli* phages and is one of the most well-studied members of the *Myoviridae* family (7). The T4 bacteriophage is a double-stranded DNA (dsDNA) virus (5) and its assembly is divided into three independent pathways: the head, the tail and the long tail fibers (LTFs) (7). The T4 bacteriophage head is composed of more than 3,000 polypeptide chains encapsulating a 172kbp dsDNA chromosome that contains 274 open reading frames which encode more than 40 structural proteins (5). This 'shell' is

**Published Online:** 20 September 2019

**Citation:** Morgan G, Lim D, Wong P, Tamboline B. 2019. Electron Microscopy to visualize T4 bacteriophage interactions with *Escherichia coli* strain DFB1655 L9, an isogenic derivative of strain MG1655 engineered to express O16 antigen. UJEMI 24:1-13

**Editor:** Julia Huggins, University of British Columbia

**Copyright:** © 2019 Undergraduate Journal of Experimental Microbiology and Immunology. All Rights Reserved.

Address correspondence to:  
<https://jemi.microbiology.ubc.ca/>

hemi-icosahedral in shape and protects the genome when the virus is transmitted between hosts (5). The bacteriophage tail is a tube-like organelle that is attached to one of the vertices of the shell and plays a critical role during infection by penetrating the cell envelope and translocating the DNA from the shell into the host (5). The LTFs are long, spindle-like fibers attached to the tail and coordinate host recognition and DNA delivery (5). Unlike animal cell viruses, infection by tailed bacteriophages, such as T4, are highly efficient due to the fact that only one bacteriophage T4 particle is required to successfully infect its host.

An understanding of phage-host interactions is of major importance from both an ecological and therapeutic standpoint due to the ability of T4 to efficiently bind and kill *E. coli* (8). In *E. coli*, outer membrane proteins (OMPs) serve as permeability channels for nutrients, toxins, and antibiotics (9). One such protein, known as OmpC, is influenced by changes in osmolarity and has been shown to be one of the surface receptors identified and bound by the T4 LTFs (9,10,11). Previous studies have highlighted the role of LPS and OmpC in the receptor function for T4 bacteriophage in *E. coli* K-12 strains. These studies have illustrated that host recognition by T4 occurs through a reversible interaction of the tip of the LTFs with LPS or with OmpC (12). Upon receptor binding to OmpC, a recognition signal is sent, causing the tail fibers to extend and irreversibly bind to the outer core region of the LPS (6).

Recent evidence suggests that *E. coli* K-12 substrain MG1655, which does not produce O16 antigen, is more vulnerable to T4 and T7 bacteriophage-induced lysis compared to *E. coli* K-12 substrain DFB1655 L9 which does produce the O16 antigen. MG1655 contains an insertion of a 1.2 kb IS5 element into the *wbbL* gene, causing disruption of the *rfb* gene cluster and resulting in an inability to produce O antigen. The *wbbL* gene encodes for rhamnose transferase, which is necessary for O antigen synthesis (13). Upon restoration of the *rfb* cluster through integration of a conjugative suicide vector pJP5603/*wbbL* into the chromosome of MG1655 upstream of the IS5 element, the DFB1655 L9 substrain is produced. DFB1655 L9 produces O16 antigen and possesses similar growth kinetics as the O16-negative MG1655 substrain (14-17).

Wachtel *et al.* explored the infection of MG1655 and DFB1655 L9 using T4 bacteriophage by quantifying the bacteriophage present within supernatant samples post-infection and found a five-fold decrease in T4 bacteriophage-specific genes compared to DFB1655 L9 supernatant (15). They concluded that the presence of O16 antigen on the surface of DFB1655 L9 strain confers resistance to T4 bacteriophage-induced lysis by decreasing adsorption of bacteriophage to the surface of *E. coli* cells. However, a follow up study conducted by Lee *et al.* performing the same protocol of infection followed by qPCR quantification of T4 and T7 specific genes did not observe such a decrease in T4 and T7 bacteriophage in the infection supernatant of MG1655 compared to the DFB1655 L9 substrain. As a result, Lee *et al.* concluded that the protection of O16 antigen-expressing *E. coli* cells from T4 bacteriophage-induced lysis was occurring via mechanisms other than decreased adsorption of the bacteriophage (16).

Given the contradictory results described above, this study aims to validate whether the presence of O16 antigen in *E. coli*, through the presence of an intact *wbbL* gene, confers protection against T4 bacteriophage-induced lysis. We hypothesize that the presence of an intact *wbbL* gene confers protection against T4 bacteriophage-induced lysis by preventing the bacteriophage from reaching the surface of *E. coli*. In line with this hypothesis, we expect that the *wbbL* deficient *E. coli* strain MG1655 will exhibit phage binding at the cell surface in electron microscopy analysis, and the strain DFB1655 L9 will not.

## METHODS AND MATERIALS

***E. coli* K-12 Substrains.** *E. coli* K-12 substrains MG1655, DFB1655 L9, and JW2203-1 were used in this study. The MG1655 and DFB1655 L9 substrains were originally obtained from the Henderson Laboratory at the University of Birmingham (14). The JW2203-1 substrain was originally obtained from the Yale Coli Genetic Stock Center as part of the Keio collection (19). Laboratory stock T4 bacteriophage (Carolina Biological, Item# 124330) was initially used to propagate T4. The MG1655 substrain was cultured on 1.5% LB agar plates. DFB1655 L9 and JW2203-1 substrains were grown on 1.5% LB agar

supplemented with 50 µg/mL kanamycin. Each substrain of *E. coli* was sub-cultured every 2 weeks by streaking isolated colonies every two weeks. All strains were grown at 37°C.

***E. coli* and T4 bacteriophage Strain Confirmation via PCR.** Single colonies were selected using a sterile pipette tip and resuspended in 40 µL dH<sub>2</sub>O. PCR reaction mixtures and thermocycling parameters were chosen according to the guidelines provided in the package insert of the Invitrogen™ Platinum™ *Taq* DNA polymerase (ThermoFisher Scientific, Cat 10966-026). *E. coli* PCR reaction mixtures were modified to include 10 µL of the diluted colony in place of 10 µL of the specified amount of dH<sub>2</sub>O and template DNA to be included in the reaction mixture. The same was done for phage strain confirmation by modifying the PCR reaction to include 5 µL of the diluted phage stock (10<sup>-1</sup>, 10<sup>-2</sup>, 10<sup>-3</sup>) in place of dH<sub>2</sub>O and template DNA to be included in the reaction mixture. Specific primer sequences used for each substrain and specific *gp23* and *gp10a* primer sequences used to identify T4 or T7 bacteriophage as well as thermal cycling parameters can be found in the supplementary information (Table S1, S2). Following colony PCR, PCR products were mixed with 1X loading buffer and run on a 1% agarose gel prepared in 1X TAE buffer with 1X SYBR Safe DNA Gel Stain. Gels were run for 1 hour at 120V, or until the dye front travelled approximately 75% of the entire gel length. Gels were subsequently imaged on the gel documentation system.

**Bacteriophage Propagation.** T4 bacteriophage propagation and clean up was performed according to the “Phage on Tap” protocol (20). MG1655 substrain was cultured overnight at 37°C with agitation at 200 RPM in 5 mL LB broth media. The overnight culture was added to 45 mL of LB broth media supplemented with 0.001M CaCl<sub>2</sub> and MgCl<sub>2</sub> and incubated with agitation at 200 RPM for 1 hour at 37°C. 100 µL of stock T4 (7.1 x 10<sup>9</sup> PFU/mL) were added following the 1-hour incubation and allowed to incubate with agitation at 200 RPM at 37°C for 5 hours or until clearing. Phage lysates were collected in sterile centrifuge tubes and kept at 4°C until cleanup.

Phage lysates were centrifuged at 4,000 x g for 20 minutes. The supernatant was carefully collected into a separate, sterile tube. The supernatant was then filter-sterilized using a 0.22 µm vacuum filter to yield a bacteria-free phage lysate. The filter-sterilized phage lysate was stored at 4°C for the remainder of the project.

**T4 Bacteriophage adsorption studies by Transmission Electron Microscopy.** *E. coli* K-12 substrains MG1655, DFB1655 L9, and JW2203-1 were imaged within the University of British Columbia Bioimaging Facility on the Hitachi H7600 TEM. Each strain was grown as an overnight culture prior to phage adsorption. T4 bacteriophage stock was added to 1 mL aliquots of each substrain at a multiplicity of infection (MOI) of approximately 10 and was incubated for 9 minutes at 37°C. The mixture was pelleted following centrifugation at 5,000 x g for 2 minutes. The supernatant was removed, removing any unadhered bacteriophage, and the pellets were resuspended in fixative solution (4% PFA, 2.5% glutaraldehyde in 1X PBS) and were allowed to fix for 15 minutes at room temperature. Cells were pelleted at 5,000 x g for 2 minutes at 4°C following fixation and were resuspended in 1X PBS, then pelleted again at 5,000 x g for 2 minutes at 4°C. This washing process with 1X PBS was repeated two more times. After the final wash, cells were resuspended in a final volume of 300 µL 1X PBS. 3 µL of each cell suspension were mounted on glow-discharge electron microscopy grid followed by the addition of 5 µL of uranyl acetate as the negative stain. Excess liquid was wicked off with filter paper after 30 seconds. Samples were then visualized under the Hitachi H7600 transmission electron microscope at varying magnifications.

**Lytic Assay.** Overnight cultures were prepared for *E. coli* K-12 substrains MG1655, DFB1655 L9, and JW2203-1 and were normalized to an OD<sub>600</sub> reading of 0.60. 125 µL of each diluted substrain was added to 96-well plates. T4 bacteriophage was either added to each sample at an MOI of 2, or the wells were topped up with LB media or LB supplemented with 50 µg/mL Kanamycin to a total volume of 200 µL per well. OD<sub>600</sub>

readings were taken every 10 minutes over a 24-hour period at 37°C with mild shaking every 10 minutes.

## RESULTS

**Verification of *E. coli* Substrains MG1655, DFB1655 L9, and JW2203-1 Using PCR and Agarose Gel Electrophoresis.** Colony PCR analysis confirmed the identity of the *E. coli* K-12 substrains MG1655, DFB1655 L9, and JW2203-1. A single specific band at 2.0 kb was observed for MG1655, corresponding to the 0.8 kb non-functional *wbbL* gene with an insertion of a 1.2 kb IS5 element (Figure 1). A prominent band was observed at 0.8 kb for DFB1655 L9 which corresponds to the size of the functional *wbbL* gene, while fainter non-specific bands are seen at 1.5 kb and 2 kb (Figure 1). These non-specific bands correspond to the single crossover event of the *wbbL* gene, generating both functional and non-functional forms of the *wbbL* gene in the DFB1655 L9 substrain, and agrees with a previous study (14). An expected single band of 1.5 kb was observed for JW2203-1, corresponding to the size of a kanamycin resistance cassette replacing the *ompC* gene (Figure 1). The expected amplification bands were observed at their respective expected molecular weights of all three *E. coli* K-12 substrains.

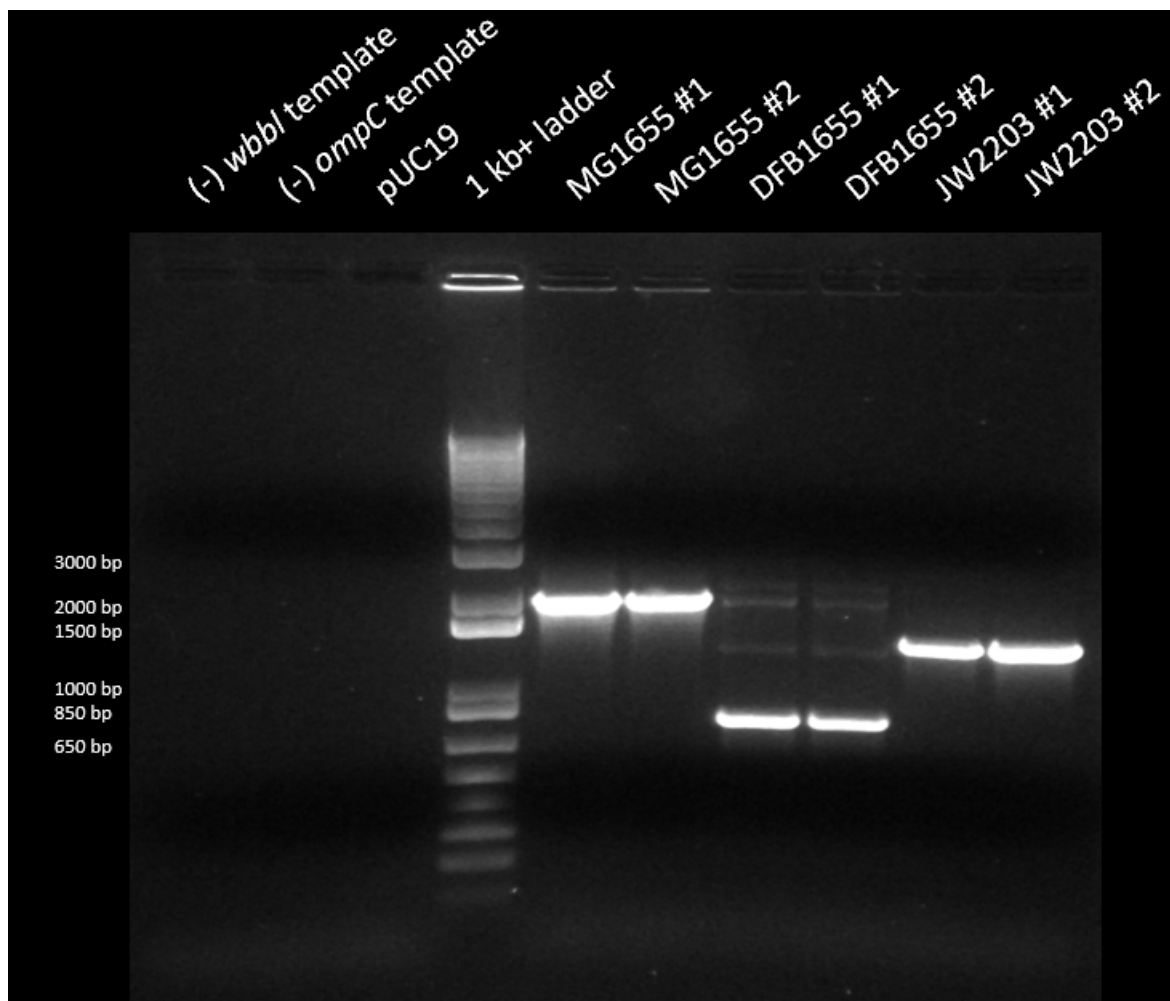


**FIG. 1** PCR analysis of *E. coli* K-12 substrains MG1655, DFB1655 L9, and JW2203-1 confirms strain genotype. PCR was performed on the 2 isolated colonies for each of MG1655, DFB1655 L9, and JW2203-1. Amplification of DNA specific regions for each of MG1655, DFB1655 L9, and JW2203-1 is expected to yield amplicons at 2 kb 0.8 kb, and 1.5 kb respectively. pUC19 was used as a positive control and is expected to yield a 189 bp amplicon, distilled water was used as a negative control which should present no bands. Amplicons were resolved on a 1% Agarose Gel at 120V in 1X TAE Buffer. Gel was prepared using Invitrogen™ UltraPure Agarose, 1X TAE buffer, and 1X SYBR™ Safe DNA Gel Stain and imaged using the AlphaImager® software on the gel documentation system.

**Verification of T4 Bacteriophage Stock Solution Purity Using PCR and Agarose Gel Electrophoresis.** PCR analysis confirmed the purity of the T4 bacteriophage stock. Figure 2 shows a 1% agarose gel of T4 bacteriophage *gp23* amplicons using primers flanking the gene *gp23*. Using the *gp23* primers, our expected amplicon size was 398 bp, and an amplicon size of approximately 400 bp was acquired, indicating that our stock contains T4 bacteriophage (Figure 2). In a separate gel, to determine whether our T4 bacteriophage stock was contaminated with T7 bacteriophage (another bacteriophage commonly used in our laboratory), primers flanking *gp10* were used. The T4 bacteriophage *gp23* PCR conditions were used as a positive control, since using pUC19 as the positive control had proven to be unsuccessful in previous gels. Our test conditions showed no bands at the expected amplicon size of *gp10* at 295 bp, indicating the absence of T7 bacteriophage from our T4 bacteriophage stock (Figure 3). For both T4 and T7 test conditions, negative controls for the template and primers were prepared using distilled water. Overall, PCR analysis was positive for T4 bacteriophage and negative for T7 bacteriophage.

**Overnight Assay of *E. coli* Substrains MG1655, DFB1655 L9, and JW2203-1 in the Presence of T4 Bacteriophage Confirms Suspected Infection Phenotypes.** To confirm previous observations regarding substrain phenotype and T4 bacteriophage infection, overnight cultures of MG1655, DFB1655 L9, and JW2203-1 were spiked with 1% (v/v) of the propagated phage stock in triplicate and were incubated at 37°C for approximately 16

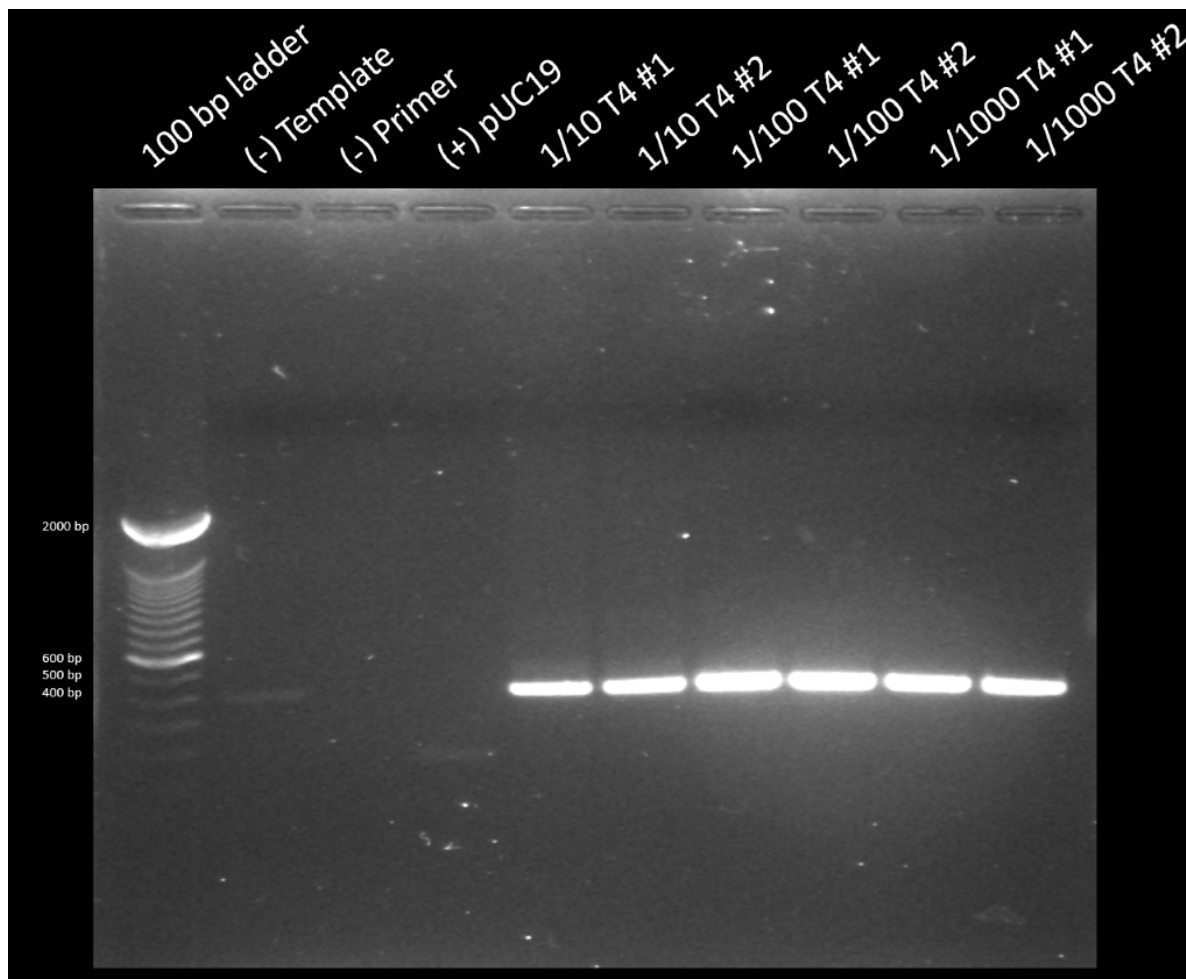


**FIG. 2** T4 *gp23* major capsid protein indicates presence of T4 bacteriophage. PCR was performed on the propagated T4 bacteriophage using primers flanking the *gp23* major capsid protein with an expected amplicon band size of 0.4kb. pUC19 was used as a positive control and is expected to yield a 189 bp amplicon and distilled water was used as a negative control which should yield no bands. Amplicons were resolved on a 1% Agarose Gel at 120V in 1X TAE buffer. Gel was prepared using Invitrogen™ UltraPure Agarose, 1X TAE buffer, and 1X SYBR™ Safe DNA Gel Stain and imaged using the AlphaImager® software on the gel documentation system.

hours. The controls containing no bacteriophage showed growth for all three substrains, indicating no phage contamination as well as cell viability of each strain (Figure S4). Growth was also observed in all phage treatments of DFB1655 L9 and JW2203-1, indicating that these strains are resistant to lysis by T4 bacteriophage. In contrast to this, no bacterial growth was seen for any replicate of MG1655 treated with phage (Figure S4), indicating that this strain is sensitive to T4 bacteriophage lysis. These results are consistent with previous observations showing that the presence of T4 bacteriophage inhibits growth of MG1655, while DFB1655 L9 and JW2203-1 appear to be more protected from infection relative to MG1655.

**Transmission Electron Microscopy Shows Greater Adherence of T4 Bacteriophage on *E. coli* K-12 MG1655 Relative to Substrains DFB1655 L9 and JW2203-1.** To visualize the interaction of T4 bacteriophage on surface of *E. coli* K-12 substrains MG1655, DFB1655 L9, and JW2203-1, transmission electron microscopy was performed. Propagated T4 bacteriophage stock was used to infect substrains at an estimated multiplicity of infection (MOI) of 10 and was incubated for 9 minutes at 37°C while shaking to maximize T4 adsorption, while preventing a full 20-minute lytic cycle from occurring. The cells were visualized upon fixation with PFA and glutaraldehyde followed by negative staining with uranyl acetate.

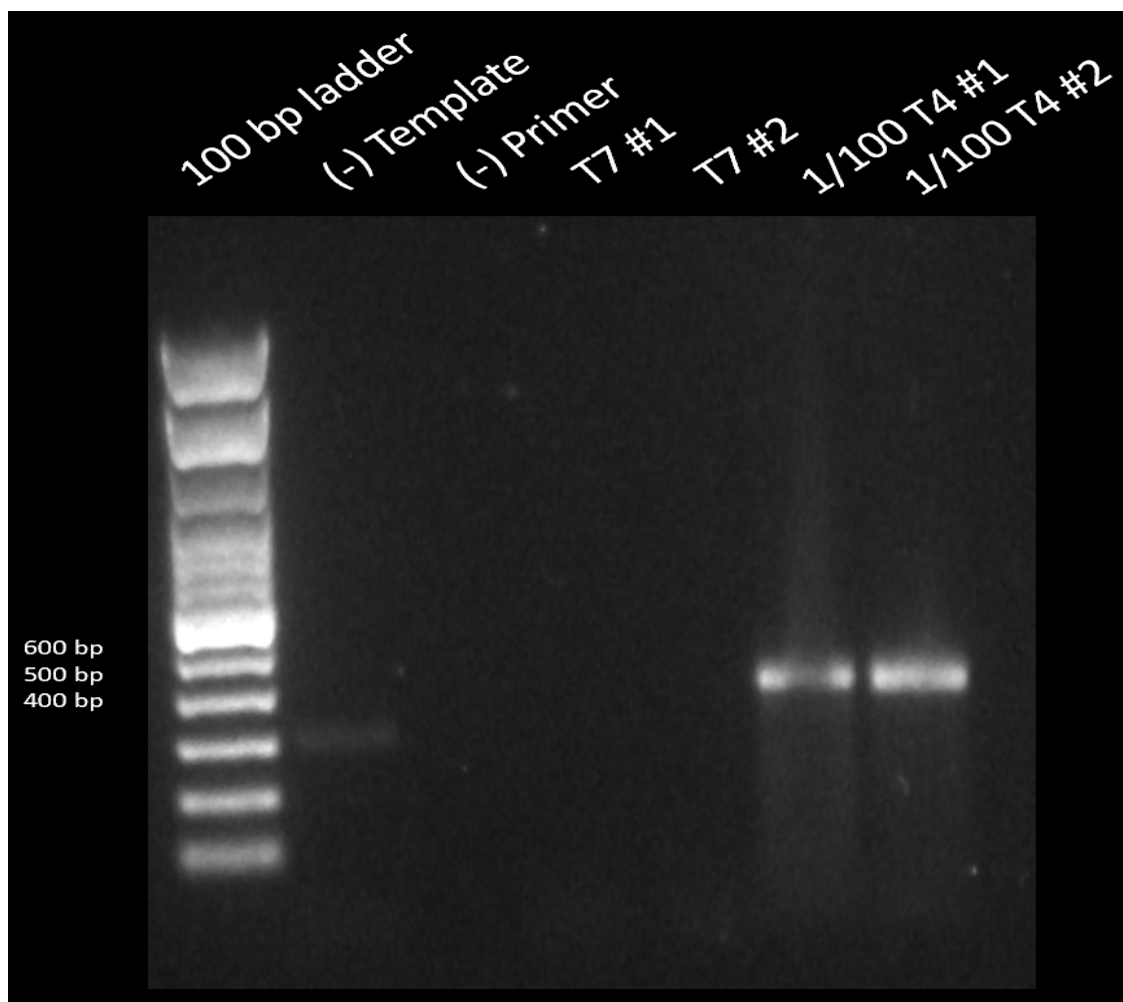


**FIG. 3** Absence of gp10a major capsid protein (T7) indicates pure T4 bacteriophage stock. PCR was performed on the propagated T4 bacteriophage using primers flanking the *gp10a* gene encoding the major capsid protein, yielding no bands. T4 bacteriophage conditions were used as a positive control and should yield a 0.4kbp amplicon and distilled water was used as a negative control which should yield no bands. Amplicons were resolved on a 1% Agarose Gel at 120V in 1X TAE buffer. Gel was prepared using Invitrogen™ UltraPure Agarose, 1X TAE buffer, and 1X SYBR™ Safe DNA Gel Stain and imaged using the AlphaImager® software on the gel documentation system.

The morphology of *E. coli* K-12 MG1655 and DFB1655 L9 appear to be similar in shape and size. Individual cells of both substrains are approximately 2-4  $\mu\text{m}$  in length and 1  $\mu\text{m}$  in width. The morphology of JW2203-1 is distinctly different from the other two substrains, as JW2203-1 cells are relatively smaller, approximately 1-2  $\mu\text{m}$  in length and 1  $\mu\text{m}$  in width, and the end tips of many JW2203-1 cells appear to be transparent (Figure S3). Bacterial layers cannot be accurately distinguished due to the nature of the negative stain method and the limited resolution power of TEM. Bacterial surface structures such as flagella or pili are observable at higher magnifications with an approximate length of 100-400 nm (Figure 4).

The detailed structure of T4 bacteriophage adsorbed to *E. coli* K-12 MG1655 was observed using TEM. Phage width and length were measured to be 90 nm and 200 nm, respectively, consistent with past studies that have examined phage morphology (7). The capsid and a cylindrical mid-section were measured to be approximately 100 nm in diameter (Figure 4). Some capsids were observed to be relatively more translucent than others. Tail fibers are observable on unbound phage (Figure 4). T4 tails were measured to be approximately 50-100 nm. Tail fibers varied in length, ranging from 25-150 nm (Figure 4A). The distinct morphology of T4 bacteriophage is clearly observable under these TEM conditions however, the resolution of bacteriophage structural features visibly decrease upon cell surface binding. In these cases, the bacteriophage capsid is the sole phage component observable on the surface of the bacterial cell.

Relative to DFB1655 L9 and JW2203-1, MG1655 showed a considerable amount of T4 bacteriophage bound to its surface. As a general estimation for the number of phage particles bound to each substrain, it appears that approximately 5-15 phage were bound to most MG1655, while approximately 0-1 phage were bound to DFB1655 L9 (Figure 5). No phage was observed to be bound to the OmpC deficient strain JW2203-1 (Figure S3).

Features of T4 bacteriophage bound to *E. coli* K-12 MG1655 under EM are shown in Figure 5A-C. In Figure 5A-B, approximately 10-15 phage capsid heads are observed to be bound to the outer surface of the cell. Some bacteriophage appears to be internalized;

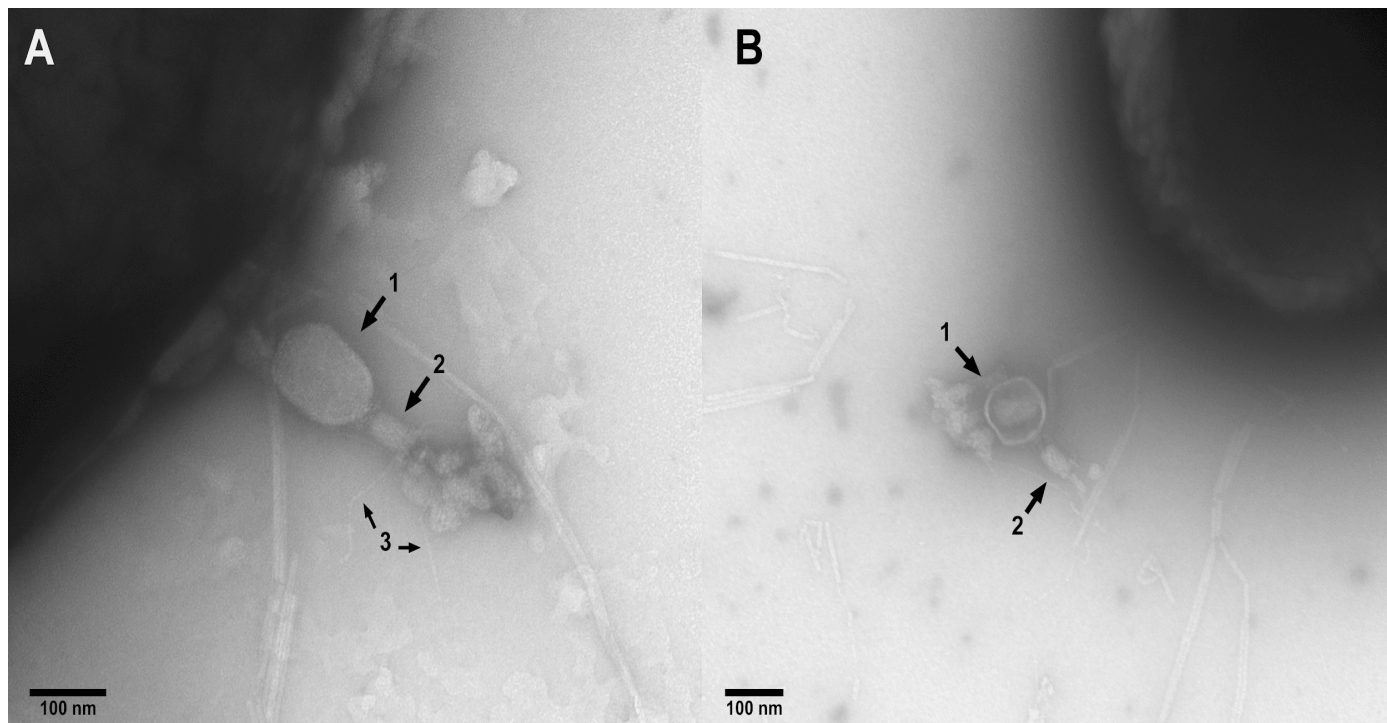


**FIG. 4** Morphology of T4 Bacteriophage – Transmission Electron Micrograph. Both images display the phage capsid (1), tail (2), and thin tail fibers (3). (A) T4 bacteriophage tail appears to be attached to extracellular component, likely cellular debris, and is facing away from an *E. coli* K-12 MG1655 cell. 200000X Magnification. (B) T4 bacteriophage appears to be attached to extracellular filament, potentially flagella or pili of *E. coli* K-12 MG1655. 150000X Magnification. Observed by using a Hitachi H7600 transmission electron microscope.

however, due to limitations in resolving depth of field with TEM, it cannot be determined whether they are internalized or bound above or below the cell. For these reasons, it is unclear where the bacteriophage that appear to be internalized within the *E. coli* cell are located. In addition, the bottom left side of the outer membrane shows a phage in an atypical orientation, where its tail sheath is directed away from the cell surface (Figure 5B). The rod-shaped *E. coli* has a distinct morphology, in which its total length is approximately 2.5  $\mu\text{m}$ , and the top portion of the cell appears to be 1.5  $\mu\text{m}$  in width while the bottom portion of the cell is narrower, being only 0.75  $\mu\text{m}$  in width (Figure 5A). Apart from phage capsids, no distinct phage morphological characteristics could be distinguished. The presence of multiple phage capsids adhered to the cell surface of MG1655 suggests that successful infection and subsequent lysis of MG1655 by T4 bacteriophage is likely to occur if incubated for longer prior to imaging. This is supported by the observations made during the phenotypic characterization of each *E. coli* substrain in the presence of T4 bacteriophage, where the growth of MG1655 was impeded due to infection by T4 bacteriophage (Figure S4). A capsid and tail structure appear to be emerging from a topographically abnormal region of the cell surface, where extracellular material can be observed between the phage capsids and the surface of the cell (Figure 5C). It was initially speculated that this image displays lysis of MG1655 by T4 bacteriophage. However, it is unclear whether this is the case, as only 9 minutes of infection had elapsed during sample preparation, while a typical T4 lytic cycle can take much longer to occur. As a result, it is possible that this image is merely depicting phage interaction with a structurally compromised *E. coli* cell. Regardless, this image clearly exhibits some interaction occurring between MG1655 and T4 bacteriophage and supports observations of interactions between

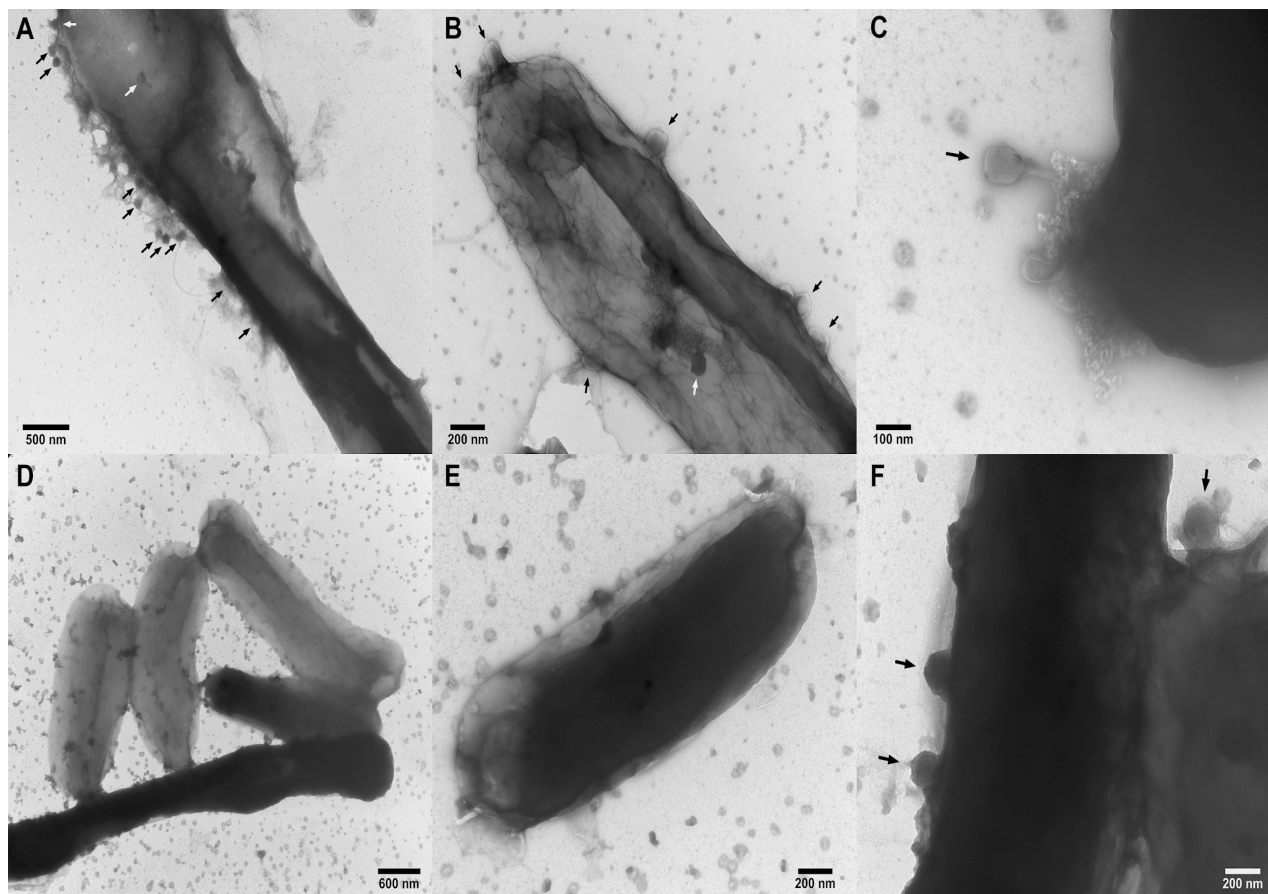


**FIG. 5** Comparison of *E. coli* K-12 MG1655 and DFB1655 L9 cells – Transmission Electron Micrograph. (A-C) Multiple phage appear to be bound to *E. coli* K-12 MG1655 as indicated by black and white arrows. (A) 40000X Magnification. (B) 80000X Magnification. (C) 150000X Magnification. (D-E) *E. coli* K-12 DFB1655 L9 are present with no phage adhered. (D) 30000X Magnification. (E) 80000X Magnification. (F) *E. coli* K-12 DFB1655 L9 appears to have three phage capsids attached to the surface. 150000X Magnification. Observed by using a Hitachi H7600 transmission electron microscope.

phage and the surface of other MG1655 cells.

*E. coli* K-12 DFB1655 L9 was visualized after incubation with T4 bacteriophage (Figure 5D-F). Figure 5D illustrates the absence of phage adherence on the cell surface of DFB1655 L9. A total of 5 rod-shaped *E. coli* with lengths of 2-4  $\mu\text{m}$  and widths of 0.6-1.2  $\mu\text{m}$  can be observed (Figure 5D). No phage were observed to be bound on the surface of these bacteria. A magnified image of *E. coli* substrain DFB1655 L9 after incubation with T4 bacteriophage is depicted in Figure 5E; similarly, T4 bacteriophage is absent from the cell surface. The cell is characteristically rod-shaped with a length of 1  $\mu\text{m}$  and width of 0.4  $\mu\text{m}$ .

Contrary to our hypothesis, T4 bacteriophage bound to *E. coli* K-12 DFB1655 L9 was observed where 3 phage capsid heads can be seen bound to the outer surface of 2 cells (Figure 5F). The cell on the left, 0.5  $\mu\text{m}$  in width and 1  $\mu\text{m}$  in length, contained two phage heads adhered to its surface. The other cell on the right side of the image contains a single phage bound to the top region. No distinct phage morphological characteristics could be distinguished with the exception of the phage head, in which two are opaque whereas the other is a translucent grey.

**Lytic Assay Demonstrates that the Presence of *wbbL* or Absence of *ompC* is Insufficient to Confer Long-Term Resistance to T4 Bacteriophage-Induced Lysis.** To compare the susceptibility of the different *E. coli* K-12 substrains, each substrain was exposed to T4 bacteriophage for a 36-hour time period and OD<sub>600</sub> measured every 15 minutes. MG1655 substrains exposed to T4 bacteriophage showed a decrease in the OD<sub>600</sub> reading overtime, which is indicative of lysis occurring (Figure 6). MG1655 substrains without exposure to T4 bacteriophage did not show such a decrease in OD<sub>600</sub>, indicating that the decrease in OD<sub>600</sub> observed when MG1655 is exposed to T4 bacteriophage is indeed due to the presence of bacteriophage, and is likely resulting in bacteriophage-induced lysis.

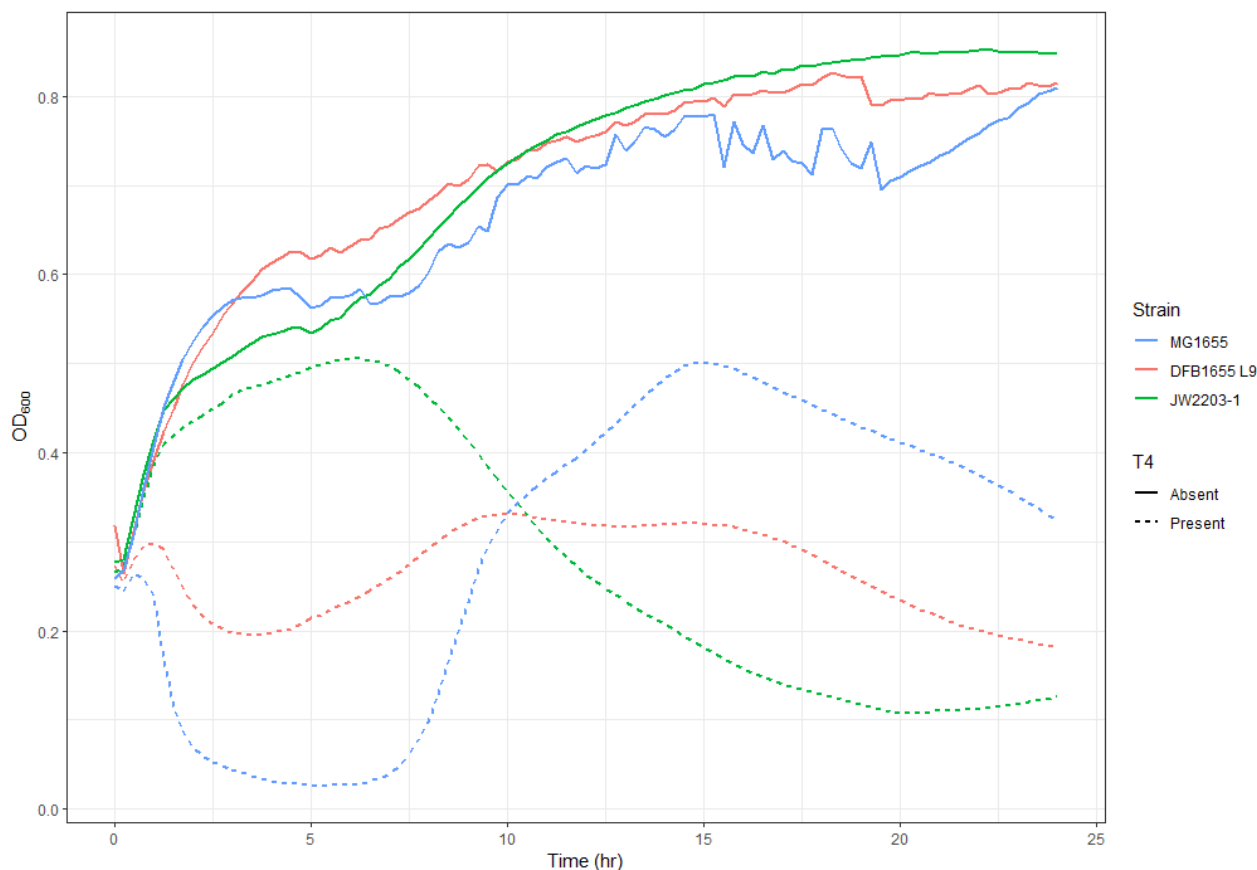


**FIG. 6** Lysis Curve of *E. coli* K-12 MG1655, DFB1655 L9, and JW2203-1 in the presence and absence of T4 bacteriophage. OD<sub>600</sub> was monitored over a 24-hour period, with readings taken at 10-minute intervals.

The difference in OD<sub>600</sub> over time between T4-positive and T4-negative samples was not observed in the DFB1655 L9 substrains (Figure 6). The OD<sub>600</sub> of the DFB1655 L9 remained steady at approximately 0.2-0.3 in the presence of T4 bacteriophage, indicating that T4 bacteriophage is, at the very least, not killing DFB1655 L9 at a increased rate relative to what can be observed for the MG1655 substrain. Substrain JW2203-1 exhibited the same extent of decrease in OD<sub>600</sub> as the MG1655 when exposed to T4 bacteriophage (Figure 6). Although T4 bacteriophage was not observed at the cell surface of JW2203-1 during the transmission electron microscopy experiments, we suspect that JW2203-1 is susceptible to T4 phage-induced lysis after long periods of exposure.

## DISCUSSION

The prevalence and importance of bacteriophage research is making a revival as scientists continue the conversation on the need for alternatives to antibiotics. The idea of phage therapy has been around for more than a century (21,-3). This idea was largely abandoned in the 1930s and 1940s following the discovery of the first antibiotic (21-23). However, following the recently successful treatment of patients infected with multidrug resistant bacteria using phage therapy (21-23), it seems to be a concept that may have been sidelined preemptively. A better understanding of the interactions between bacteriophage and bacteria is the key to elucidating the mechanism of how phages mediate successful bacterial infection, and ultimately, the design of efficient phage therapies. In addition to understanding phage-host interactions, specific methods of host immunity to bacteriophage are also critical in developing effective therapies. Ultimately, an increased understanding of phage-host interactions and host immunity to infection is necessary for scientists to pursue the biotechnological advancements that expand the potential efficacy of phage therapy in combating the crisis of multidrug resistant bacteria.

Transmission electron microscopy experiments were carried out to investigate whether the presence of an intact *wbbL* gene confers protection against T4 bacteriophage-induced lysis by preventing the bacteriophage from reaching the surface of *E. coli*. We predicted that the *wbbL* deficient *E. coli* strain MG1655 would exhibit phage binding at the cell surface in electron microscopy analysis, and the strain DFB1655 L9 would not. In addition, we hypothesized that the strain JW2203-1  $\Delta ompC$  would be resistant to T4 bacteriophage-induced lysis, as it is deficient in the expression of OmpC, a key receptor presumed to be involved in T4 adsorption (10). Our expectations varied from our findings, as outlined in our results. Although, T4 could be observed bound to MG1655 in high numbers, EM images revealed T4 bound to a single DFB1655 L9 cell. In addition to these findings, MG1655, DFB1655 L9, and JW2203-1 all displayed decreased growth characteristics in the presence of T4 phage after long periods of exposure. Overall, our results show that DFB1655 L9 and JW2203-1 have increased protection against T4 infection and adsorption upon initial exposure to the virus, but they are not immune, as presented in our lysis curve assay.

While *E. coli* K-12 substrain DFB1655 L9, which possesses a rescued *wbbL* gene, has been observed to have resistance to T4 and T7 bacteriophage-induced lysis, the exact mechanisms that confer such resistance are not fully understood (15,16). Previous studies have shown the importance of LPS for host recognition by T4 through interactions of LTF tips with LPS followed by short tail fiber binding to the outer core region of the LPS (6,12). However, research investigating whether the obstruction of the LPS by the presence of O16 antigen protects against phage adsorption has been contradictory (15,16).

Given the notable differences in the number of phages present on the surface of each of the different *E. coli* substrains, conclusions can be drawn regarding the susceptibility of each strain to T4 bacteriophage infection. As indicated in the results, most of the MG1655 cells were found to have more than 5 phage at their cell surface, while only a single DFB1655 L9 cell appeared to have phage interactions on its surface. Since only a single DFB1655 L9 cell was observed to have phage adhered to its surface, it is unclear whether DFB1655 L9 is indeed susceptible to T4 bacteriophage-induced lysis, or whether this observation indicates that DFB1655 L9 is merely susceptible to T4 adherence, but not infection. Similarly, it may also be the case that O16 antigen is present on LPS in variable amounts across the entire surface of the cell, and in this single DFB1655 L9 cell, O16

antigen was not confluent in LPS over the full surface of the *E. coli* cell. Also, given this single instance of T4 adherence on DFB1655 L9, it may also be possible that this particular DFB1655 L9 cell had a mutation that reduced the level of O antigen expression thereby rendering the cell susceptible to attack. Whether this is due to an adherence mechanism at the cell surface involving the O16 antigen requires further investigation.

Based on our EM images, we expected to see similar results when carrying out a lytic assay with MG1655, DFB1655 L9, and JW2203-1, with MG1655 having relatively higher levels of T4 bacteriophage-induced lysis and DFB1655 L9, and JW2203-1 having little or no apparent lysis. In the presence of T4 phage, substrain MG1655 had a rapid decrease in OD<sub>600</sub> after 1 hour of T4 exposure. This trend was not observed in MG1655 where T4 was absent. However, after 7 hours, the OD<sub>600</sub> of the MG1655 strain began to recover to greater values than what was initially seen, suggesting the development of resistance against T4 phage. Interestingly, we also observed suppressed and decreased cell growth for DFB1655 L9 and JW2203-1, respectively. Similarly, to MG1655, DFB1655 L9 displayed a decrease in OD<sub>600</sub> after 2 hours, where this trend was not observed when T4 was absent. Following depression of growth, the OD<sub>600</sub> of DFB1655 L9 begins to recover after 5 hours to values slightly above the initial OD<sub>600</sub>. We suspect that this trend depicts DFB1655 L9 possessing heightened immunity to initial T4 infection, and possibly, its ability to develop complete resistance to T4 phage-induced lysis faster than MG1655. Finally, JW2203-1 in the presence of phage displayed a noticeable decline in OD<sub>600</sub> after 7 hours, which was not observed in JW2203-1 absent of T4. It may be that T4 bacteriophage does not require the presence of OmpC to adhere to *E. coli* and can adhere to the surface of these bacteria through the use of some other anchoring system given enough time. The delayed OD<sub>600</sub> decrease in the JW2203-1 strain compared to the MG1655 substrain may be explained by the lack of an “anchor” in the form of OmpC but remaining susceptible through chance encounters and another adsorption mechanism. Another possibility is that the OmpC protein is not required for receptor function when the K-12 strain possesses the Bstrain-type LPS that has a glucose residue at the distal end (12), and thus, after subsequent replications of T4, the phage may have evolved to have high affinity to the cells absent of OmpC although less likely due to time constraints.

Observations made regarding the morphology of T4 bacteriophage in Figure 4 included the fact that phage tail fibers were frequently broken off of the phage. This may have been a result of the sample preparation process or could possibly be a part of the molecular interaction between *E. coli* cells and the phage during infection (24). Additionally, the differences in capsid morphology, such as the differences in transparency between phage (Figure 4, 5) may be the result of differences in the stage of infection of a given phage. For instance, T4 capsids that are more opaque, as seen in the phage attached to DFB1655 L9 (Figure 5), are speculated to still contain their genomic content; more transparent capsid heads, as seen in Figure 4, are speculated as having already injected their DNA into the cell.

**Conclusions** Our study investigated the effect that the presence or absence of an intact *wbbL* gene, and the subsequent expression of O16 antigen on the surface of *E. coli* has on the resistance of *E. coli* to T4 bacteriophage-induced lysis. Through our results we conclude that the presence of an intact *wbbL* gene, as well as the deletion of *ompC*, do appear to confer resistance to T4 bacteriophage-induced lysis. Fewer phage were observed on the surface of DFB1655 L9 cells in comparison to MG1655 when viewed under TEM. A lytic experiment shows that DFB1655 L9 and JW2203-1 do indeed possess increased resistance to lysis by T4 bacteriophage relative to MG1655, however the exact mechanism that mediates this resistance still remains unclear.

**Future Directions** Given the nature of our project and the limited time and resources, enumerating the number of phage particles adhered to the surface of *E. coli* K-12 MG1655, DFB1655 L9, and JW2203-1 was unfeasible. Using the transmission electron microscopy sample preparation methods and guidelines outlined in this paper, it may be possible for future studies to accurately count the number of phages adhered by reproducing our results in a shorter time frame. This would both provide further support to the observations made in this paper, as well as provide concrete evidence that the quantity of phage able to adhere to

the surface of each strain does indeed differ. Additionally, given the results of the lysis assay, an interesting next step would be to use transmission electron microscopy to visualize the interaction between *E. coli* K-12 substrains and T4 bacteriophage at different stages of infection. Since our study mainly focused on the initial infection prior to a single lytic cycle, it is unclear whether the number of phage able to adhere to and infect *E. coli* varies over a longer period of time. Maintaining infected cultures and fixing them at specific time points for imaging may provide useful data regarding changes to the quantity of phage adherence and infection.

Because the single DFB1655 L9 cell observed to have phage adhered to its surface was not reproducible by us within the same sample nor during a separate sample preparation and imaging session, future studies should also look into whether this result is a property of DFB1655 L9 or is merely an anomalous result arising from sample preparation. Additionally, the notable morphology differences observed between JW2203-1 and the other substrains of *E. coli* K-12 tested in this study presents another potential research avenue that future papers may pursue. These observed morphological differences may implicate differences in the structural integrity of JW2203-1, thus making this strain more susceptible to biological stressors such as the build-up of toxins, and as a result, impairing its growth.

## ACKNOWLEDGEMENTS

We would like to give thanks to the Department of Microbiology and Immunology at the University of British Columbia for providing the opportunity as well as the funding necessary for us to carry out this project. We are grateful to both Dr. David Oliver and Reynold Calderon for their continued guidance and support throughout the entirety of our project. We would also like to thank the UBC Bioimaging Facility, in particular Dr. Miki Fujita and Brad Ross, for allowing us to use and providing support with the Hitachi H7600 TEM. Lastly, we would also like to recognize Team 1-Delta: Jaspreet Gill, Karen Lau, Tina Lee, and Hasel Lucas, for collaborating with us and allowing us to use their supplies and equipment throughout our project.

## CONTRIBUTIONS

All team members contributed equally to the project proposal, planning of experiments, and lab work.

## REFERENCES

1. **Silhavy T, Kahne D, Walker S.** 2010. The bacterial cell envelope. *Cold Spring Harb Perspect Biol.* A000414
2. **Rakhuba DV, Kolomiets, EI, Dey, ES, Novik, GI.** 2010. Bacteriophage receptors, mechanisms of phage adsorption and penetration into host cell. *POL J MICROBIOL.* **59**:145.
3. **Reeves P, Cunneen M.** 2010. Biosynthesis of O-antigen chains and assembly. *Microbial Glycobiology* 319-335.
4. **Wang L, Wang Q, Reeves PR.** 2010. The Variation of O Antigens in Gram-Negative Bacteria. *Subcellular Biochemistry* 123-152.
5. **Leiman PG, Kanamaru S, Mesyanzhinov VV, Arisaka F, Rossmann MG.** 2003. Structure and morphogenesis of bacteriophage T4. *Cell. Mol. Life Sci.* **60**:2356–2370.
6. **Bartual SG, Otero JM, Garcia-Doval C, Llamas-Saiz AL, Kahn R, Fox GC, Raaij MJ van, King JA.** 2010. Structure of the bacteriophage T4 long tail fiber receptor-binding tip. *Proceedings of the National Academy of Sciences of The United States of America* **107**:20287–20292.
7. **Yap ML, Rossmann MG.** 2014. Structure and function of bacteriophage T4. *Future Microbiology* **9**:1319–1327.
8. **Bryan D, El-Shibiny A, Hobbs Z, Porter J, Kutter EM.** 2016. Bacteriophage T4 infection of stationary phase *E. coli*: life after log from a phage perspective. *Frontiers in Microbiology* **7**.
9. **Liu Y-F, Yan J-J, Lei H-Y, Teng C-H, Wang M-C, Tseng C-C, Wu J-J.** 2012. Loss of Outer Membrane Protein C in *Escherichia coli* Contributes to Both Antibiotic Resistance and Escaping Antibody-Dependent Bactericidal Activity. *Infect. Immun.* **80**:1815–1822.
10. **Washizaki A, Yonesaki T, Otsuka Y.** 2016. Characterization of the interactions between *Escherichia coli* receptors, LPS and OmpC, and bacteriophage T4 long tail fibers. *PeerJ* **5**:1003–1015.
11. **Sato M, Machida K, Arikado E, Saito H.** 2000. Expression of outer membrane proteins in *Escherichia coli* growing at acid pH. *Appl. Environ. Microbiol* **66**:943-947.

12. **Yu F, Mizushima S.** 1982. Roles of lipopolysaccharide and outer membrane protein OmpC of *Escherichia coli* K-12 in the receptor function for bacteriophage T4. *J. Bacteriol* **151**:718–722.
13. **Stevenson G, Neal B, Liu D, Hobbs M, Packer NH, Batley M, Redmond JW, Lindquist L, Reeves P.** 1994. Structure of the O antigen of *Escherichia coli* K-12 and the sequence of its rfb gene cluster. *J. Bacteriol* **176**:4144–4156.
14. **Browning D, Wells T, França F, Morris F, Sevastyanovich Y, Bryant J, Johnson M, Lund P, Cunningham A, Hobman J, May R, Webber M, Henderson I.** 2013. Laboratory adapted *Escherichia coli* K-12 becomes a pathogen of *Caenorhabditis elegans* upon restoration of O antigen biosynthesis. *Mol. Microbiol.* **87**:939-950.
15. **Wachtel A, Guo A, Sagorin Z, Etti E.** 2017. Serotype O Antigen Expression in *Escherichia coli* K-12 May Confer Resistance Against T4 Bacteriophage Infection by Preventing Adsorption. *JEMI+* **3**:70-79
16. **Lee S, de Bie B, Ngo J, Lo J.** 2018. O16 Antigen Confers Resistance to Bacteriophage T4 and T7 But Does not Reduce T4/T7 Adsorption in *Escherichia coli* K-12. *JEMI* **22**
17. **Biparva N, Ghazizadeh A, Thomas H, Sun S.** 2019. Negative Stain Electron Microscopic Analysis Suggests O Antigen Expression in *Escherichia coli* strain K-12 May Prevent T4 Interactions with the Bacterial Surface. *JEMI*
18. **Furukawa H, Mizushima S.** 1982. Roles of cell surface components of *Escherichia coli* K-12 in bacteriophage T4 infection: interaction of tail core with phospholipids. *J Bacteriol.* **150**:916-924.
19. **Baba T, Ara T, Hasegawa M, Takai Y, Okumura Y, Baba M, Datsenko KA, Tomita M, Wanner BL, Mori H.** 2006. Construction of *Escherichia coli* K-12 in-frame, single-gene knockout mutants: the Keio collection. *Mol Syst Biol* **2**:1-11
20. **Bonilla N, Rojas MI, Netto Flores Cruz G, Hung S-H, Rohwer F, Barr JJ.** 2016. Phage on tap—a quick and efficient protocol for the preparation of bacteriophage laboratory stocks. *MicrobiologyOpen* **4**:2261.
21. **Sousa JAM de, Rocha EPC.** 2019. Environmental structure drives resistance to phages and antibiotics during phage therapy and to invading lysogens during colonisation. *SciRep* **9**:1–13.
22. **Lin DM, Koskella B, Lin HC.** 2017. Phage therapy: An alternative to antibiotics in the age of multi-drug resistance. *World J Gastrointest Pharmacol Ther* **8**:162–173.
23. **Botka T, Pantůček R, Mašlaňová I, Benešik M, Petráš P, Růžičková V, Havlíčková P, Varga M, Žemličková H, Koláčková I, Florianová M, Jakubů V, Karpíšková R, Doškař J.** 2019. Lytic and genomic properties of spontaneous host-range Kayvirus mutants prove their suitability for upgrading phage therapeutics against staphylococci. *SciRep* **9**:1–12.
24. **Firtel M, Beveridge TJ.** 1995. Scanning probe microscopy in microbiology. *Micron.* **26**:347-362.